INTERACTION OF LASER RADIATION WITH MATTER. LASER PLASMA

PACS numbers: 42.62.Cf; 52.58.Ns; 28.52.Av
DOI: 10.1070/QE2000v030n05ABEH001734

Neutron yield in conic targets with additional laser fuel heating

I G Lebo

Abstract. The compression and the thermonuclear energy release in conic targets with additional laser heating are calculated. It is shown that irradiation of conic targets with a compound (long plus short) KrF laser pulse with energy 300 – 400 kJ can provide a neutron yield of $\sim 10^{16}$ per shot and, accordingly, target energy gain coefficients above 0.1.

1. Introduction

The physics of laser-driven compression of thermonuclear fusion in conic targets has been studied in many papers [1 – 7]. Because of the deformation of walls near the vertex of a conic target and the thermal flux to the wall, the efficiency of energy transfer from the laser-accelerated layer of condensed material, the so-called pusher, to the fuel proves to be significantly lower for these target designs than for spherical targets subject to uniform heating. This circumstance accounts for the scepticism which has arisen around the use of conic targets in laser fusion research.

Basov et al. [7] have discussed possible target designs of a hybrid fusion-fission reactor [8 – 16]. In reactors of this type, the bulk of the useful energy will be produced owing to the fission of nuclei of heavy elements (uranium) while the fusion neutrons produced as a result of laser-driven microexplosions will permit control of the fission process.

Fig. 1 shows the energy cycle of a laser fusion power plant, where η is the laser efficiency, G is the energy gain in the target (the ratio between the released fusion energy and the laser energy absorbed in the target), M is the energy gain in the reactor, $K = (0.2 + 0.8M)G$ is the net reactor gain, E_L is the laser pulse energy, f is the pulse repetition rate, $(1/\eta - 1)E_L$ is the energy loss in the laser pumping, β the efficiency of thermal-to-electric power conversion in the reactor, $W_b = \beta W_t$ is the so-called gross reactor power, and $W_t = KfE_L$ is the thermal power.

Note that approximately 80% of the liberated energy resides in the fusion neutrons. This energy can be substantially (M times) increased owing to the fission of heavy nuclei in the reactor blanket, whereas the remaining 20% of the energy, which resides in charged particles and radiation, will be absorbed by the first reactor wall. The gross power is expended to maintain the operation of the laser

I G Lebo P N Lebedev Physics Institute, Russian Academy of Sciences, Leninskii pr. 53, 117924 Moscow, Russia

Received 21 May 1999
Kvantovaya Elektronika **30** (5) 409 – 415 (2000)
Translated by E N Ragozin, edited by M N Sapozhnikov

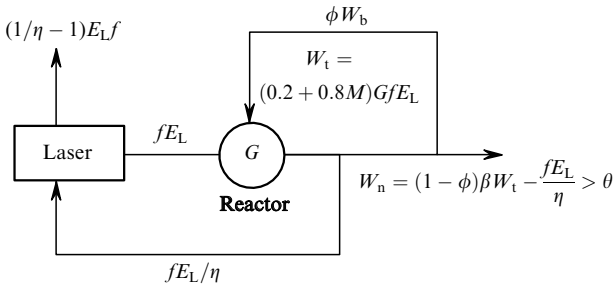

Figure 1. Schematic diagram of the energy cycle of a fusion power plant.

driver (fE_L/η) and for the inherent needs of the reactor — circulation of the heat carrier, evacuation, maintenance of safety systems, etc. (ϕW_b, where ϕ defines the consumption of power to keep the reactor running). The remaining part of the power (the net power W_n) will be supplied to consumers (a good fraction of the energy dissipated as heat during laser pumping may prove to be useful for warming and other necessities). Clearly, the closure of the energy cycle of the plant requires that the condition $W_n > 0$ be satisfied. It is assumed that $\beta = 0.4$ and $\phi = 0.1 - 0.2$.

We emphasise: For a gain in the blanket $M = 10$ and $\phi = 0.2$, the requirement on the efficiency of the laser-target system is of the form $G\eta \geqslant 0.4$. If the gain $M \geqslant 1000$ is attainable in the blanket (see Refs [14 – 16]), then $G\eta \geqslant 0.004$, which permits the requirements on the laser – target system to be considerably alleviated.

To date, impressive advances have been made in the development of a high-power neodymium laser for the initiation of a fusion 'burst' in a spherical target [17]. However, the question of whether a laser of this type can operate under reactor conditions remains open.

A gas excimer KrF laser has several advantages (a wavelength four times shorter than for a Nd laser, a broad amplification band, a relatively high efficiency, the capability to operate in a repetitively pulsed mode, and the potential of obtaining up to 500 kJ per pulse from one module). However, the formation of a 5 – 10 ns pulse required to compress spherical targets calls for the realisation of a complex and costly optical system.

An important prerequisite to the operation of a hybrid reactor is the ignition of fusion microbursts by the smallest possible number of beams (ideally, by one beam). This is due to the fact that the major portion of the surface of the first wall will be occupied by fuel elements containing fissionable materials. In this connection, Basov et al. [7] discussed the possibility of using conical targets for these hybrid reactors, which would allow the irradiation of the target with one

or two beams. For targets with internal energy input, a one- or two-beam laser system can also be employed. In this case, however, short pulses approximately 100 ps in length will be required [7].

The present work is concerned with the physics of compression of KrF-laser-irradiated conic targets studied on a basis of one- and two-dimensional numerical calculations. The feasible neutron yield from these targets for an energy of 0.3 – 2 MJ is estimated, and the major problems and their possible solutions are discussed.

For several reasons, detailed numerical simulation of the entire problem of the acceleration and compression of thermonuclear fuel in conical targets using present-day computers is troublesome. The length of the conic channel in targets of this type should be of the order of 1 cm, while the thickness of a laser-accelerated pusher should be 10 – 50 μm, with the heating and the fusion energy liberation taking place on a 100 – 500 μm scale. The densities of the walls, the pusher, and the internal gas will differ by a factor of 10^5 – 10^6, the gas volume changing by several orders of magnitude. Under these conditions, the problem simulation is conveniently performed in Lagrangian coordinates. In this case, however, it is difficult to take into account the slipping of the pusher and of gas layers relative to the walls and the attendant evaporation of the conical target and formation of a boundary layer.

In principle, the use of Eulerian coordinates allows us to include the above effects, but simulating the entire process necessitates very large computer resources (random-access memory and computer speed). In this connection two approaches are used: (i) the Lagrangian technique, which permits the inclusion of the heating and the compression of the thermonuclear fuel, the energy redistribution between the fuel and the cone bottom, taking into account different equations of state of the matter (EOS) in each of the subdomains, etc.; (ii) the Eulerian technique to model the pusher acceleration in the channel, taking the energy redistribution between the subdomains and the evaporation of the walls of the conic target into account.

2. Simulation of conic target compression

As already mentioned, in the compression of material in conic targets, the efficiency of energy deposition to the thermonuclear fuel is significantly lowered due to the deformation of walls at the cone vertex. With the use of the one-dimensional DIANA code [18], a long series of calculations (over 50) was performed to simulate the compression of quasi-spherical conic targets.

The one-dimensional DIANA code enables us to numerically solve the equations of gas dynamics in the Lagrangian coordinates, of electron and ion heat transfer, and of the kinetics of fusion reactions, assuming that charged particles are absorbed in the same cell from where they originate, while the neutrons are free to escape from the computation range. The EOS take into account the electron degeneracy in the compressed plasma and the corrections for 'elasticity' of multiply charged ions [19].

In the calculations, it was assumed that the cone walls are perfectly smooth, absolutely elastic, and thermally insulated. The power of the laser pulse built up linearly with time up to the point $t_1 = 100$ ns, and the pulse energy E_L was varied from 0.2 to 2 MJ for an external radius R_0 and an apex angle Θ_0. The pusher in the form of an aluminium or polyethylene segment of thickness Δ_1 resided at the cone base. Inside the cone at a distance R_1 from the vertex lay the layer of deuterium-tritium ice or low-density porous polymer material containing a liquid DT mixture of mass M_f. A gold layer of radius R_2 resided in the central region to account for the losses due to the deformation of the cone bottom. The target cavities were filled with DT gas of density 0.01 – 0.1 mg cm^{-3}.

The design of a target of this type is shown in Fig. 2a. The parameters R_0, Δ_1, M_f,, and R_1 were varied. With the aid of simulations, the first two parameters were selected so that the pusher would commence deceleration by the end of the laser pulse (i.e. the instant of maximum fuel compression in different simulation versions ranged from 96 to 104 ns). The speed of pusher motion and the efficiency of energy transfer to the fuel rise as the cone radius increases and the initial pusher thickness decreases — as with spherical shell targets (see, e.g. Ref. [20]). Using spherical targets as an analogy, we introduce the notion of a shell aspect ratio $A_s = (R_0 - R_2)/\Delta_1$.

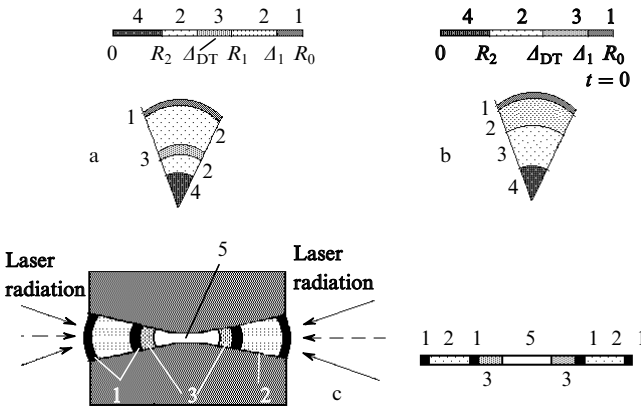

Figure 2. Designs of conic laser targets: a two-stage target (a), a two-layer target (b), and a double target for counter-propagating beams (c): (1) shell of aluminium or polyethylene; (2) DT gas; (3) internal shell (layer of condensed DT fuel or porous polymer containing a liquid DT mixture); (4) layer of gold or lead; (5) vacuum.

Within the framework of the model under consideration, the gain of conic targets will depend on the laser energy deposition E_L and the aspect ratio A_s. In addition, it will depend on the ratio between the lateral radii of the foot ($r_1 = 0.5R_0\Theta_0$) and the vertex ($r_2 = 0.5R_2\Theta_0$) of the conic target: $\varepsilon = r_1/r_2 = R_0/R_2$. (Generally speaking, this dependence will be more complex, because non-one-dimensional effects are disregarded in our model.) The existence of a central dense target region ($r \leqslant R_2$) results in a significant reduction of the neutron yield compared to the results obtained when this region was missing. Fig. 3a – 3c shows the laser and target parameters with (version 1, Fig. 3b) and without (version 2, Fig. 3c) the central region. The density (Fig. 3d) and ion temperature (Fig. 3e) distributions at the instant of peak fuel compression are also given. The neutron yield was 10^{15} in version 1 and 10^{17} in version 2.

The results of four simulations of conic two-stage targets with different parameters are collected in Table 1. In the calculations, it was assumed that $\Theta_0 = \pi/4$. An approximate dependence of the gain G in these targets on the E_L, A_s, and ε parameters was obtained to generalise the results of

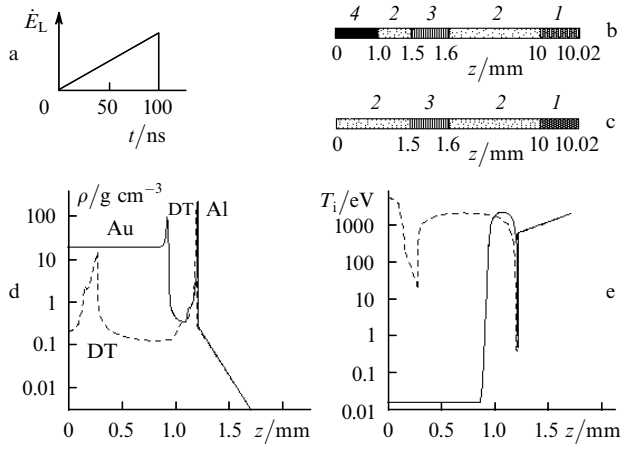

Figure 3. Formulations of the problem and results of one-dimensional numerical simulations for a KrF laser with $E_L = 300$ kJ – temporal pulse shape (a), parameters of conic targets, versions 1 (b) and 2 (c), density (d) and ion temperature (e) z-axis distributions at the instant of peak compression for Versions 1 (solid line, the neutron yield $Y_n = 10^{15}$) and 2 (dashed line, $Y_n = 10^{17}$): (1) shell of aluminium or polyethylene; (2) DT gas; (3) internal shell; (4) layer of condensed DT fuel or porous polymer containing a liquid DT mixture.

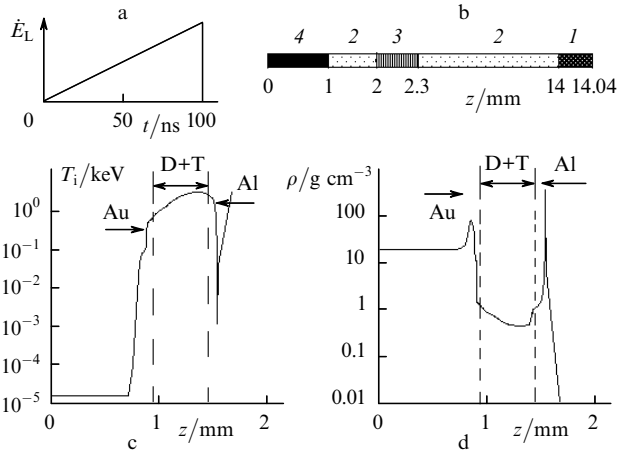

Figure 4. Formulation of the problem and results of one-dimensional numerical simulation of a conic target for a KrF laser with $E_L = 2$ MJ: temporal pulse shape (a), parameters of a conic target (b), ion temperature (c) and distributions of the density (d) along the z-axis at the instant of peak compression (the neutron yield $Y_n = 2 \times 10^{17}$, the gain $G = 0.25$): (1) aluminium or polyethylene shell; (2) DT gas; (3) inner shell (layer of condensed DT fuel or porous polymer containing a liquid DT mixture; (4) gold layer.

Table 1.

E_L/MJ	R_0/cm	R_1/cm	R_2/cm	Δ/μm	Δ_{DT}/μm	Y_n (10^{16})	G
0.3	1.2015	0.21	0.1	15	100	0.15	0.014
0.3	1.26156	0.21	0.126	15.6	100	0.0091	0.0085
2	1.4035	0.22	0.1	35	200	11	0.15
2	1.4435	0.22	0.14	35	200	3.1	0.04

simulations:

$$G \approx 0.01(E_L/300\ \text{kJ})^{0.75}(A_s/330)^{0.8}(\varepsilon/10)^{4.5}. \quad (1)$$

It is evident that the gain depends rather strongly on the ε parameter, and a value $G \sim 0.1$ is attainable for $\varepsilon = 10$, $A_s = 370$, and $E_L = 2$ MJ.

Note that experiments with spherical shells having a high aspect ratio were staged in the USSR and Japan (see Refs [20, 21]; the shells were shown to survive at least the acceleration stage and their velocities to be as high as 200 – 300 km s^{-1}. Lebo et al. [22] discussed the feasibility of accelerating dense thin layers in cylindrical and conic targets to velocities over 100 km s^{-1} employing a KrF laser. The feasibility of accelerating layers in conic channels to velocities greater than 40 km s^{-1} was demonstrated [6] employing a neodymium laser with an intensity of $(3 - 5) \times 10^{12}$ W cm^{-2} and a pulse length of ~ 30 ns.

Fig. 4 depicts the formulation of the problem and the results of one-dimensional simulations of conic target compression for a driver energy of 2 MJ (a 100% absorption of the laser radiation was adopted in all instances). The distributions of density and temperature over the axis of a compressed target at the instant of collapse are shown in Fig. 4c, d. One can see that the fuel is compressed to a density of 1 – 2 g cm^{-3} (Fig. 4d) and the temperature amounts to 1 – 5 keV (Fig. 4c).

Along with a two-stage target of this type, also considered were targets in which the fuel is frozen onto the inside of the pusher or in which the shell is made of a light porous material filled with a liquid DT mixture (see Fig. 2b). In these targets, there occurs a separation of the heavier materials and the fuel in the course of acceleration towards the centre, the denser inert materials finding themselves at the top and being entrained by the evaporation wave. For two-component single-stage targets, in the context of our model, the dependence of gain on the target parameters is about the same as for two-stage targets. Be it as it may, the neutron yield is approximately 10^{15} for an energy of about 300 kJ (i.e., $G \sim 0.01$) and amounts to 10^{17} for $E_L = 2$ MJ.

Clearly, the requisite gain $G \geqslant 0.1$ in conic targets can be obtained for driver energies $E_L \geqslant 1 - 2$ MJ. The use of two-sided conic targets (see Fig. 2c) can somewhat augment the neutron yield for a given energy input but complicates the driver design, because two counter-propagating beams synchronised in time will be required rather than one.

The laser efficiency in the mode of 100-ns pulse production may be relatively high. Thus, the chances that a neutron yield of the order of $10^{16} - 10^{17}$ will be attained for an energy deposition of 1 – 2 MJ are good despite the fact that similar neutron yields can, in principle, be obtained in the nanosecond pulse mode for significantly lower driver energies, provided the symmetry of irradiation is high (see, e.g., Refs [23, 24]).

3. Calculations of the neutron yield from conic targets with additional laser heating of the DT fuel

Zvorykin et al. [25] and Lebo et al. [26] discussed the feasibility of augmenting the neutron yield in conic targets irradiated by a combined (long plus short) KrF laser pulse. The scheme considered in these papers is based on the idea of separate heating and compression of the target (see also Refs [27 – 30]). The feasibility of designing a KrF laser generating composite pulses was considered (the first pulse with a length $\tau_1 \sim 100$ ns and an energy $E_1 \sim 300 - 400$ kJ and the second one with a length $\tau \sim 10 - 20$ ps and an energy

$E_2 \sim 20 - 30$ kJ). A laser of this type could have an efficiency of about 5–10% in the long pulse and up to 1% in a train of short pulses and could operate in the pulse-periodic mode at a pulse-repetition rate of the order of 1 Hz. Upon meeting these requirements and attaining a neutron yield from the target of $\sim 10^{16} - 10^{17}$ per shot, this laser could serve as a driver in a hybrid fusion-fission reactor.

Zvorykin et al. [25] presented the design of a two-stage cryogenic conic target studied earlier as applied to a KrF laser driver [7] and assessed the feasibility of increasing the neutron yield through additional heating effected by a short laser pulse. This work concentrates on two-dimensional numerical calculations of the neutron yield in conic targets heated by a double pulse. A one-stage, two-component target is more suited to such pulses because inert layers will be vaporised in the acceleration stage and the second (short) pulse will penetrate directly into the fuel.

A conic target with an apex angle $\pi/4$ had a radius of 12.206 mm; a 6 μm aluminium shell (the pusher) was located at the cone base. A 100-μm-thick layer of the DT fuel was frozen on the inside of the pusher, and the central target region with a radius of 1 mm was made of gold. As before, the laser power built up linearly with time for 100 ns and the absorbed energy of the laser pulse was 300 kJ. In our calculations, the cone walls were assumed to be perfectly elastic, smooth, and thermally insulated.

The target compression was calculated employing a two-dimensional Lagrangian ATLANT code in spherical axially symmetric coordinates r and θ [31]. This code took advantage of the same physical model as the one-dimensional DIANA code. The target and laser pulse parameters are given in Fig. 5. The cone apex angle was equal to $\pi/4$. The long laser pulse ($\tau_1 = t_1 = 100$ ns) was triangular-shaped in time and delivered an energy of 300 kJ, while the short one ($\tau_2 = t_3 - t_2 = 10$ ps), an energy of 20 kJ. The laser radiation power was prescribed by the formula

$$q(t, \theta) = q_1(t) q_2(\theta),$$

where q_1 and q_2 are the functions that respectively describe the temporal and angular dependences of the laser power, with

$$\int q_2(\theta) \sin\theta \mathrm{d}\theta = 1.$$

The calculations were performed assuming the radiation intensity of the first pulse to be either independent of the angle ($q_2 = \text{const}$) or Gaussian-shaped with $\theta_0 = \pi/8$:

$$q_2(\theta) = \frac{\exp[-\theta/\theta_0)^2]}{C_1},$$

where C_1 is the normalisation factor for the first pulse.

In the latter case, the shell was subjected to deformation during its flight to the centre. Owing to a strong distortion of the Lagrangian cells, attempts to bring the simulations to the instant of deceleration were not successful (a strong distortion of the Lagrangian cells can be regarded as the disruption of the pusher). Therefore, we can conclude that a highly uniform irradiation of the pusher is required. Be that as it may, the pusher ruptures during acceleration in the channel when the intensities of the incident laser radiation at the axis and at the periphery of the layer differ by a factor of 2–3 (in the following section, we set out the results of two-dimensional simulations accomplished on a Eulerian grid, which take into account the deformation of the channel walls and bear out this conclusion).

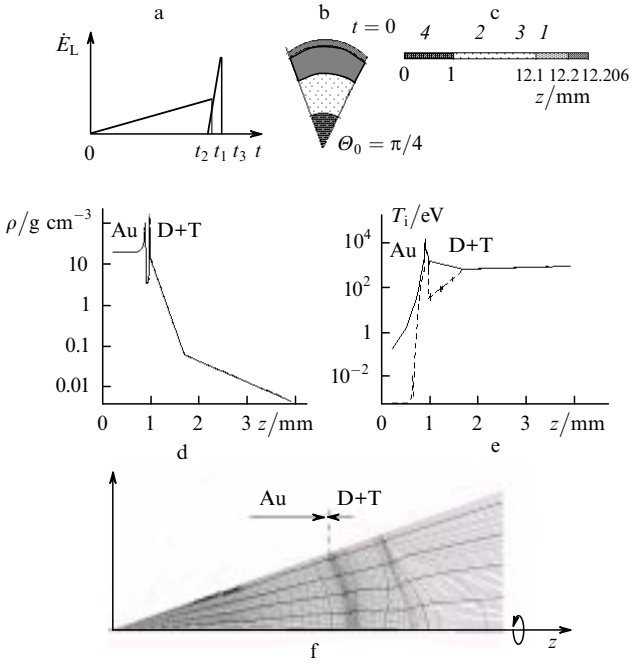

Figure 5. Formulation of the problem and results of numerical simulation of the conic target compression by the double pulse of a KrF laser for an energy of the first pulse $E_1 = 300$ kJ, an energy of the second one $E_2 = 20$ kJ, and $\lambda_z = 0.1$ g cm^{-2}: temporal shape of the double pulse (a), shape (b) and parameters of the conic target along the axis (c), density (d) and ion temperature (e) distributions along the z-axis for $t_2 = 91.533$ ns (dashed lines) and $t_3 = 91.543$ ns (solid lines), and also Lagrangian lines in the compressed portion of the conic target for $t_2 = 92.43$ ns (f).

The target heating by the second pulse was modeled as follows: The radiation was allowed to reach the surface on which the density assumed the critical value and then penetrated into the target being absorbed according to the law $\sim \exp(-\int \rho \mathrm{d}z/\lambda_z)$, where z is the distance measured from the critical surface; $\lambda_z = \rho z$ is the effective depth of radiation penetration. The angular dependence of the power of the second laser pulse was of the form

$$q_2(\theta) = \frac{\exp[-(\theta/\theta_0^{(2)})^2]}{C_2},$$

where C_2 is the normalisation factor for the second pulse. In the test version, the intensity of the second pulse, as of the first one, did not depend on the θ angle but penetrated a depth $\lambda_z = 0.1$ g cm^{-2}. In this case, the neutron yield increased twofold.

In subsequent versions, the angular dependence of the laser pulse was described by a Gaussian, and the parameters λ_z and $\theta_0^{(2)}$ were varied. The second stage of the process was modeled beginning from the point in time t_2, with the distributions of the gas dynamic target parameters obtained for $q_2 = \text{const}$ for the first pulse. Simulations were performed in which the intensity of the second pulse was angle-independent and with the angular dependence of the type $\theta_0^{(2)} = \pi/16$ for $\lambda_z = 0.1$, 0.02, and 10^{-4} g cm^{-2}. The calculations for $\theta_0^{(2)} = \pi/16$ and $\lambda_z = 0.02 - 0.1$ g cm^{-2} modeled the possibility of transfer of the short-pulse energy to the interior of the target due to 'suprathermal' particles and 'channeling'

[29, 30], while those for $\lambda_z = 10^{-4}$ g cm^{-2} the energy transfer by shock waves [27].

Fig. 5 shows the results of simulations for $\lambda_z = 0.1$ g cm^{-2}: the distributions of density (Fig. 5d) and ion temperature (Fig. 5e) along the cone axis at the points in time $t_2 = 91.533$ ns (the dashed lines) and $t_3 = 91.543$ ns (the solid lines). The temperature rises steeply under the action of the second pulse while the density is hardly affected. The neutron yield builds up during compression and subsequent plasma expansion.

In comparison with the versions devoid of the second pulse, the neutron yield increased by a factor of 5–10 to become as high as $(1-3)\times 10^{16}$ owing to additional fuel heating. In this case, the yield was higher when the additional energy was deposited in the bulk than in the version where the energy of the second laser pulse was absorbed near the critical surface.

Note also that the mass of DT fuel in conical targets was taken to be high, so that the radiation of the second pulse was knowingly inputted into the DT fuel. Generally speaking, the mechanism of separation of the dense inert layers and the fuel in the course of shell acceleration calls for additional investigation. Should it prove to be efficient, it will be possible to replace a part of the fuel mass by an equal mass of an inert material to save tritium.

4. Some considerations concerning unsolved problems

Note that several important points were omitted in this paper. First is the effect of cone walls on the stability of the layer flight. The walls of actual targets are not perfectly elastic. Some layers can slide past one another, from which may arise the Kelvin–Helmholtz instability. Furthermore, the wall material will vaporise by the action of laser radiation and thermal flux, which may be responsible for the 'screening' of laser radiation (see, e.g., Ref. [32]). Second, the effect of small-scale structure of the laser beam was not included (see, e.g., Ref. [33]). Third, the mechanism of interaction and penetration of a short ultrahigh-power pulse into a dense above-critical plasma has not been studied. All of these points demand serious numerical and experimental investigations.

The effect of heating nonuniformity on the motion of shells and the buildup of hydrodynamic instabilities are currently central problems in the study laser fusion. A considerable body of experimental and theoretical information has already been accumulated, making it possible to predict the influence of the above effects on the target gain G as a function of the intensity and the nonuniformity of laser irradiation, and also on the compression ratio of the thermonuclear fuel in the heating of spherical targets by a nanosecond laser pulse. The relevant data for the irradiation of conic targets by 100 ns laser pulses are missing. In our opinion, the feasibility of stable acceleration of thin layers in cylindrical and conic channels can be studied with modern equipment, which deliver pulses with energies of the order of 100 J [34], with recourse to two-dimensional numerical simulations to interpret the resulting data.

Given below are two versions of the calculations modeling the acceleration of a polyethylene layer of initial thickness 50 μm and density 1 g cm^{-3} in a copper 1.5-mm-long cylindrical channel with an internal radius of 80 μm. The KrF laser pulse energy was 120 J. The radiation power increases linearly with time up to 100 ns and has the form $q(r,t) = q_1(t)q_2(r)$. In the first version of calculation,

$$q_2(r) = \frac{\exp\left[-(r/R_f)^2\right]}{C},$$

where $C = 0.5\pi R_f^2\left\{1-\exp\left[-(R_0/R_f)^2\right]\right\}$; $R_0 = 120$ μm is the radius of the right boundary of the computation range; and $R_f = 80$ μm is the effective radius of the focal spot (see Fig. 6).

Simulated in the second version was an 'ideal focus,' when $q_2(r) = 1/\pi R_f^2$ for $r \leqslant R_f$ and $q_2(r) = 0$ for $r > R_f$. Unlike the previous series of calculations, this one was made with recourse to the Eulerian two-dimensional NATCY code (r and z coordinates) [35]. Invoking the Eulerian method allows us to take into consideration the slipping of the shell relative to the channel walls and the forced distortion and the vaporisation of the walls themselves. Among the drawbacks of the method are the necessity of using a finite-difference scheme with a small spatial increment (fractions of a micrometer), which requires a large random-access memory and is associated with a large consumption of the processor time to calculate the shell flight in a long channel.

Fig. 6 displays the calculated plasma isodensity contours at the points in time $t = 27.4$ ns and the density distributions along the channel axis for $t = 22.4$ and 27.4 ns. It is evident that the pusher had been ruptured under the action of a 'Gaussian' beam by the point in time 27 ns and the density at the axis had gone below the critical density; the cylindrical channel had melted at edges. The laser-pulse intensity distribution in the case involved was substantially nonuniform and the difference of the temperatures at the axis and the cone wall-pusher interface was about 300%. Note that, given these irradiation nonuniformities, spherical targets are also ruptured upon when they fly through a distance far shorter than its initial radius.

Fig. 7a (at the left) shows the plasma isodensity contours at the point in time 27.4 ns for version 2. Given in Figs 7b and 7c (at the right) are the density distributions along the channel axis at the points in time 27.4 and 47.4 ns and also the plot of

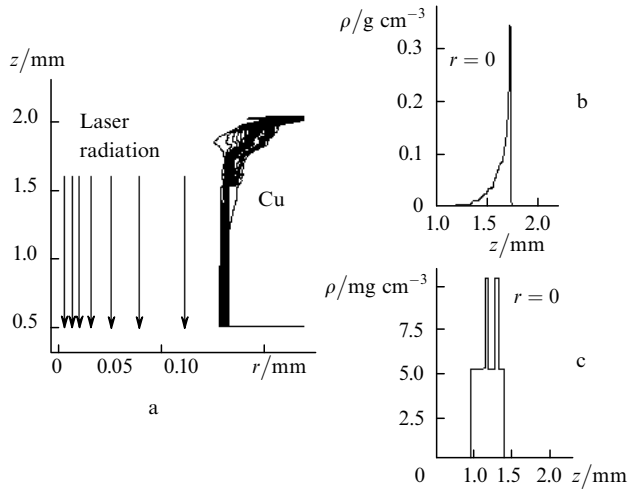

Figure 6. Results of two-dimensional numerical simulation of the polyethylene layer acceleration in a cylindrical channel driven by a KrF laser having a 'Gaussian' intensity distribution: isodensity lines at $t = 27.4$ ns (a) and the density distribution along the z-axis at $t = 22.4$ (b) and 27.4 ns (c).

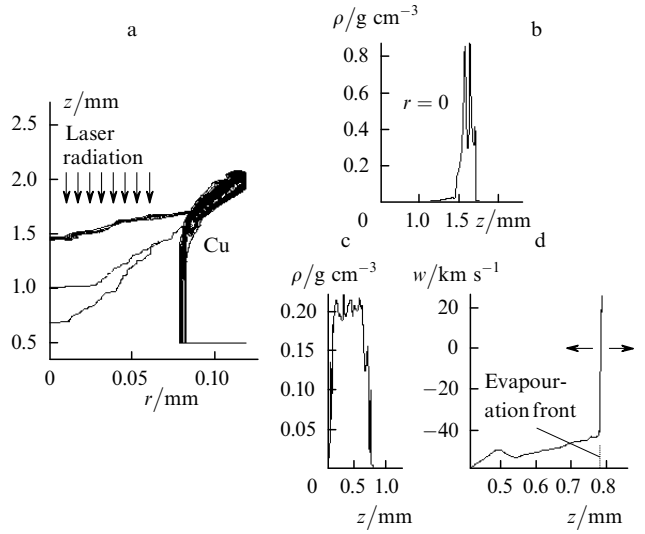

Figure 7. Results of two-dimensional simulations of the polyethylene layer acceleration in a cylindrical channel driven by a KrF laser with a constant intensity distribution for $r < 80$ μm (the channel radius): isodensity contours at the point in time $t = 27.4$ ns (a), density distributions along the z-axis for 27.4 (b) and 47.4 ns (c) (the layer has flown out of the channel), and also the distribution of the longitudinal velocity component at $t = 47.4$ ns (d).

the longitudinal component of the plasma velocity w at 47.4 ns (Fig. 7d). By this time, the dense plasma layer reaches the channel end and flies outwards. The plasma bunch velocity is 50 km s^{-1} for a channel length of 1.5 mm. It was not possible to calculate the pusher flight through a channel approximately 1 cm in length because limitations were imposed by the computer resources. However, it is easily estimated that the layer velocity in the channel that long would exceed 100 km s^{-1} for the given parameters of the laser pulse. It is significant that the layer retains a rather high density (over 0.2 g cm^{-3}) in its flight and is capable of imparting an appreciable specific momentum ($P \sim 10^{13} - 10^{14}$ erg cm^{-3}) to the obstacle. The bunch deceleration is accompanied by the intense emission of radiation.

5. Basic results and conclusions

Therefore, the inclusion of losses due to deformation of the cone walls and bottom results in a significant lowering of the fuel temperature and neutron yield. A high irradiation uniformity is required to ensure a stable layer acceleration in a conic channel approximately 1 cm in length driven by a laser pulse with a duration of the order of 100 ns (specifically, in the event of a conventional Gaussian intensity distribution, the pusher ruptures upon flying through no less than 1 mm). In the case of additional laser heating of the fuel, a gain $G \geqslant 0.1$ can be attained in conic targets for a KrF laser pulse energy of $\sim 300 - 400$ kJ. This signifies that it is possible to attain the G values basically proximate to those predicted for spherical targets irradiated by a 'sharpened' nanosecond laser pulse [24].

Given the virtues listed above, the KrF laser is, in our opinion, a candidate for the driver of a hybrid thermonuclear reactor. Present-day laser facilities with pulse energies of 100-1000 J can be used to investigate the stability of thin-layer acceleration in channels, which is a currently central problem in any branch of inertial confinement fusion research.

Acknowledgements. The author would like to express his gratitude to V D Zvorykin and V B Rozanov for valuable discussions of the results of this work.

References

1. Vovchenko V I, Gerasimov A S, et al. Pis'ma Zh. Eksp. Teor. Fiz. **26** 628 (1977)
2. Taran M D, Tishkin V F, Favorskiĭ A P, Feoktistov L P O Modelirovanii Skhlopyvaniya Kvazisfericheskikh Misheneĭ v Tverdotel'nykh Konusakh (On the Simulation of Collapse of Quasi-Spherical Targets in Solid-State Cones) Preprint (Moscow: Keldysh Institute of Applied Mathematics, Academy of Sciences of the USSR, 1980)
3. Gamaliĭ E G, Lebo I G, Rozanov V B Preprint No. 97 (Moscow: Lebedev Physics Institute, Academy of Sciences of the USSR, 1981)
4. Borovskiĭ A V, Korobkin V V Kvantovaya Elektron. (Moscow) **8** 5 (1981) [Sov. J. Quantum Electron. **11** 1 (1981)]
5. Demchenko V V, Chukbar K V Fiz. Plazmy **16** 496 (1990)
6. Fizicheskie Protsessy v Obolochechnykh Konicheskikh Misheneyakh (Physical Processes in Conic Shell Targets) Tr. Inst. Obshcheĭ Fiz. Akad. Nauk SSSR **36** (1992)
7. Basov N G, Lebo I G, Rozanov V B, Tishkin V F, Feoktistov L P Kvantovaya Elektron. (Moscow) **25** 327 (1998) [Quantum Electron. **28** 316 (1998)]
8. Feoktistov L P, Avrorin E N, et al. Kvantovaya Elektron. (Moscow) **5** 349 (1978) [Sov. J. Quantum Electron. **8** 201 (1978)]
9. Basov N G, Sheindlin A E, et al. Izv. Akad. Nauk SSSR, Ser. Energetika i Transport (2) 3 (1979)
10. Basov N G, Grigoriants R R, Isakov A I, Kalmikov Yu K, Kartashov K V, Komin A V, Krivosheev M V, Lebo I G, Maksimenko B P, Merkul'ev Yu A, Rozanov V B, Finkelshteĭn K I, Charitonov V V, Sherstnev K B Preprint No. 214 (Moscow: Lebedev Physics Institute, Academy of Sciences of the USSR, 1983)
11. Basov N G, Belousov N I, Grishunin P A, Kalmykov Yu K, Lebo I G, Rozanov V B, Sklizkov G V, Subbotin V I, Finkel'shteĭn K I, Kharitonov V V, Sherstnev K B Kvantovaya Elektron. (Moscow) **14** 2068 (1987) [Sov. J. Quantum Electron. **17** 1324 (1987)]
12. Adamov E O, Basov N G, Ganev I Kh, Davydov V K, Lebo I G, Rozanov V B, Khmel'shchikov V V, Khryastov N A, Cherkashov Yu M Preprint No. 72 (Moscow: Lebedev Physics Institute, Academy of Sciences of the USSR, 1988)
13. Adamov E O, Basov N G, Ganev I Kh, Davydov V K, Lebo I G, Rozanov V B, Khmel'shchikov V V, Khryastov N A, Cherkashov Yu M Preprint No. 73 (Moscow: Lebedev Physics Institute, Academy of Sciences of the USSR, 1988)
14. Basov N G, Subbotin V I, Feoktistov L P Vestn. Ross. Akad. Nauk **63** 878 (1993)
15. Feoktistov L P Matematicheskoe Modelirovanie **7** 41 (1995)
16. Basov N G, Feoktistov L P Technical Program and Abstracts of the XXIVth European Conference on Laser Interaction with Matter, Madrid, 1996, H3-1
17. McCrory R L Technical Program and Abstracts of the XXVth European Conference on Laser Interaction with Matter (Formia, Italy, 1998)
18. Zmitrenko N V, Karpov V Ya, Fadeev A P, Shpatakovskaya G V, Shelaputin I I Vopr. At. Nauki i Tekhn. Ser. Metody i Programmy Chislennogo Resheniya Zadach Matematicheskoi Fiziki (2) 38 (1983)
19. Afanas'ev Yu V, Gamaliĭ E G, Rozanov V B Tr. Fiz. Inst. Akad. Nauk SSSR **134** 10 (1982)
20. Gus'kov S Yu, Danilov A E, Zakharenkov Yu A, Lebo I G, Mikhaĭlov Yu A, Rozanov V B, Rupasov A A, Sklizkov G V, Fedotov S I, Shikanov A S Kvantovaya Elektron. (Moscow) **14** 2288 (1987) [Sov. J. Quantum Electron. **17** 1458 (1987)]
21. Yamanaka C Laser and Particle Beams **8** 3 (1990)
22. Lebo I G, Rozanov V B, Shpatakovskaya G V, Zvorykin V D J. Russ. Laser Res. **18** 147 (1997)

23. Afanas'ev Yu V, Volosevich P P, Gamaliĭ E G, et al. Tr. Fiz. Inst. Akad. Nauk SSSR **134** 167 (1982)
24. Bel'kov S A, Dolgoleva G V Kvantovaya Elektron. (Moscow) **25** 49 (1998) [Quantum Electron. **28** 46 (1998)]
25. Zvorykin V D, Lebo I G, Rozanov V B Kratk. Soobshch. Fiz. (9) 20 (1997)
26. Lebo I G, Rozanov V B, Zvorykin V D Proc. SPIE Int. Soc. Opt. Eng. **3683** 152 (1998)
27. Shcherbakov V A Fiz. Plasmy **9** 409 (1983)
28. Feoktistov L P In: Budushchee Nauki (The Future of Science) (Moscow: Znanie, 1985) (18) p. 168
29. Basov N G, Gus'kov S Yu, Feoktistov L P J. Sov. Laser Res. **13** 390 (1992)
30. Tabak M, Hammer J, Glynsky M E, Kruer W L, et al. Phys. Plasmas **1** 1636 (1994)
31. Lebo I G, Popov I V, Rozanov V B, Tishkin V F, Preprint No. 2 (Moscow: Lebedev Physics Institute, Russian Academy of Sciences, 1993); J. Russ. Laser Res. **15** 136 (1994)
32. Lebo I G, Nikishin V V, Rozanov V B, Tishkin V F Fiz. Plazmy **26** (5) (2000)
33. Ivanov V V, Kutsenko A V, Lebo I G, et al. Zh. Eksp. Teor. Fiz. **116** 1287 (1999)
34. Bakaev V G, Vadkovskiĭ A D, Danilov E O, et al. Kvantovaya Elektron. (Moscow) **21** 7 (1994) [Quantum Electron. **24** 5 (1994)]
35. Lebo I G, Nikishin V V, Rozanov V B, Tishkin V F Proceedings of the Sixth International Workshop on the Physics of Compressible Turbulent Mixing (Marseille, France, IUSTI, 1997) p. 312